Supporting Information

Azzarelli et al. 10.1073/pnas.1415403111

SI Methods

Practical Considerations and Limitations of the Proposed Sensing Strategy. Nine practical considerations and limitations should be taken into account before attempting to implement this sensing strategy. (*i*) Not all materials are rf-transparent. Therefore, the technique can be compromised by the presence of materials that are rf-opaque or reflect rf radiation. (*ii*) CARDs cannot be stacked on top of one another (see the discussion in *Methods*, *Binary Logic for Chemical Discrimination Using Arrays of CARDs*). (*iii*) NFC relies on inductive coupling and therefore the technique is sensitive to its magnetic environment. (*iv*) The technique, as described in *Methods*, *Method for Determining Reflection Coefficient and Readability of CARDs with a Smartphone*, is sensitive to the relative orientation of and distance between the smartphone and CARD. (*v*) Based on our findings, the on/off threshold is dictated by the amplitude of power transfer between the smartphone and the CARD. Therefore, the make and model of the smartphone may influence the on/off threshold. (*vi*) Based on our findings, the on/off threshold is dependent on the PENCIL material. (*vii*) The chemiresponsive materials used in this study are unprotected from the atmosphere of the laboratory and their performance may degrade over time. (*viii*) Because the sensing element is exposed, the behavior of the chemiresistor may change abruptly if touched or otherwise disrupted. (*ix*) This technique is demonstrated in the controlled setting of a laboratory. In a nonlaboratory setting, human and environmental exposure to nanomaterials would have to be addressed with packaging around the sensing element.

General Materials and Methods. SWCNTs (purified ≥95% as SWCNT) were kindly provided by Nano-C, Inc. HFIPN (CAS 2092-87-7) was purchased from SynQuest. NH_3 (1% in N_2) was custom-ordered from Airgas. All NFC tags used in this study (hereafter referred to generically as "NFC tag") were Texas Instruments HF-I Tag-It 13.56-MHz rf identification transponder square inlays (RI-I11-114A-01), purchased from DigiKey.

Choice of Tags. This study uses commercially available Texas Instruments HF-I Tag-It Plus Transponder Inlays (TI-Tag) to demonstrate the concept of converting a commercially available NFC tag into a chemical sensor. These tags were chosen based on their chemically robust substrate, absence of protective polymeric coating over the circuitry, commercial availability, and low cost. The electronic circuitry of the unmodified tags is supported via polyurethane glue on both sides of a thin (47-μm), flexible sheet of polyethylene terephthalate, which also serves as a dielectric layer for the capacitor. The circuit comprises an aluminum antenna that serves as an inductor (L), a parallel-plate aluminum capacitor (C), and a silicon-based IC chip (R), all connected in parallel, forming an *LCR* resonant circuit (Fig. 1).

Choice of Analytes. The selective detection of a target chemical analyte is a necessary requirement for any functional ultra-low-cost distributed chemical sensor. We achieve this requirement in a manner that does not use extensive data analysis or computationally intensive interpretation and achieves selectivity toward analytes by harnessing established properties of chemiresponsive materials (1, 2). We targeted detection of ammonia (NH_3) gas and vapors of cyclohexanone ($C_6H_{10}O$), hydrogen peroxide (H_2O_2), and water (H_2O) as model analytes for the detection of industrial, agricultural, and safety hazards. NH_3 is commonly emitted in industrial and agricultural settings and is toxic at relatively low levels (3). Cyclohexanone is a volatile organic compound, commonly used for recrystallization of explosives, such as RDX (4), that can also aid their detection (5). H_2O_2 can be used in improvised explosive devices, as a commonly used industrial reagent, and is routinely used for sanitization in hospitals.

Choice of Smartphone. We use an off-the-shelf smartphone to demonstrate the capability for wireless chemical sensing. This type of detector would be compatible with a highly distributed network of sensors accessible to a large number of people. In this context, the SGS4 was chosen as the primary NFC-enabled smartphone as a result of two factors: (*i*) At the time of this study, the Samsung Galaxy series are among the most widely distributed "smart" mobile devices in history and (*ii*) the SGS4 runs on Android, one of the most widely distributed operating systems that supports NFC applications. The demonstrated wireless chemical sensing via NFC is applicable to other NFC-enabled devices (Fig. S1). The NFC chip comprises an antenna for inductive coupling with NFC tags, a transmission module with microcontroller for 13.56-MHz carrier signal generation and tag signal demodulation, as well as embedded and external [subscriber identity module (SIM) card] security elements. When used with unmodified TI-tags, the SGS4 can read tags at ∼5 cm standoff distance through solid, nonmetallic objects such as paper, plastic, and liquids (Fig. S1).

Choice of Smartphone Application. The NFC Reader (Adam Nybäck) and NFC TagInfo (NFC Research Lab) applications were used to read the tags and were freely available from the Google Play Store at the time of this study. These applications were chosen because they display the tag's UID without invoking other time- or energy-intensive functions of the smartphone. For the purposes of this study, the tag is considered on or readable if the UID can be retrieved within 5 s or less of holding the smartphone at ∼2.5 cm distance away from the tag. Conversely, the tag is considered off or unreadable if the UID cannot be retrieved under the same conditions.

Instrumental Analysis. We monitored the rf signal response of the modified TI-tags and smartphone antennas from 10 to 20 MHz, as well as the smartphone-transmitted rf signal, with a custom-made loop probe connected via a BNC cable to a vector network analyzer (VNA) (Agilent E5061B) by measuring reflection coefficient (S_{11}) at 50 Ω port impedance and 0 dBm input power (Fig. S4).

Ball Milling. Cyclohexanone sensing material was generated by solvent-free ball milling of SWCNTs with HFIPN using an oscillating mixer mill (MM400; Retsch GmbH) within a stainless steel milling vial (5 mL) equipped with a single stainless steel ball (7 mm in diameter). The milling vial was filled with HFIPN (96 mg) and SWCNTs (24 mg) and the mixture was ball-milled for 5 min at 30 Hz.

Fabrication of PENCILs. PENCILs were fabricated by loading powdered sensing material into a steel pellet press (6-mm internal diameter) (SDS6; Across International) and compressing the powder by applying a constant pressure of 10 MPa for 1 min using a hydraulic press (MP24A; Across International).

Fabrication of Loop Probe. Hollow copper tubing covered in heat-shrink wrap was shaped into a square (5 × 5 cm) shape and soldered to a BNC adapter. Heat-shrink wrap was placed over

the connection point and was shrunk using a heat gun in a fume hood.

Dilution of Ammonia. Delivery of controlled concentrations of NH_3 to the sensing devices placed within a gas chamber was performed using a Smart-Trak Series 100 (Sierra Instruments) gas mixing system at total flow rates between 0.50 and 10.00 L/min. NH_3 was diluted with N_2.

Dilution of Vapors. Delivery of controlled concentrations of cyclohexanone vapors to the sensing devices placed within the gas chamber was carried out using Precision Gas Standards Generator Model 491M-B (Kin-Tek Laboratories). Cyclohexanone was diluted with N_2 at total flow rates of 0.25–0.50 L/min.

Gas Chamber. A custom gas chamber was fabricated by inserting two plastic syringes (1 mL; NORM-JECT), one on either side, in the bottom corners of a zippered plastic bag (1 L) and sealing it with electrical tape.

Detection of NH_3. Sensor tag data were collected according to the method described above. The sensor tag was kept on the benchtop of a fume hood for 10 min, followed by exposure to NH_3 in N_2 (35 ppm) in a gas chamber for 5 min, followed by removal and placement on a benchtop of a fume hood for 10 min. This procedure was repeated three more times; after the fourth cycle, the sensor tag was allowed to sit on the fume hood benchtop for an additional 10 min.

Detection of a Single Exposure of N_2 (Negative Control). Sensor tag data R_s and readability by SGS4 was determined according to the method described above. The sensor tag was kept on the benchtop of a fume hood for 10 min, followed by exposure to N_2 in a gas chamber for 5 min, followed by removal and placement on the fume hood benchtop for 20 min.

Detection of a Single Exposure of NH_3. Sensor tag data were collected according to the method described above. The sensor tag was kept on the benchtop of a fume hood for 10 min, followed by exposure to NH_3 in N_2 (4 ppm or 35 ppm) in a gas chamber for 5 min, followed by removal and placement on the fume hood benchtop for 20 min.

Detection of a Single Exposure of $C_6H_{10}O$. Sensor tag data were collected according to the method described above. The sensor tag was kept on a benchtop underneath a ventilation snorkel for 10 min, followed by exposure to cyclohexanone ($C_6H_{10}O$) in N_2 (335 ppm) in a gas chamber for 5 min, followed by removal and placement on a benchtop underneath a ventilation snorkel for 20 min.

Detection of a Single Exposure of H_2O_2. Sensor tag data were collected according to the method described above. The sensor tag was kept on the benchtop of a fume hood for 10 min, followed by exposure to H_2O_2/H_2O (P_{eq}) in a plastic zippered bag containing an open jar of H_2O_2/H_2O (35%) for 5 min, followed by removal and placement on the fume hood benchtop for 20 min.

Detection of a Single Exposure of H_2O. Sensor tag data were collected according to the method described above. The sensor tag was kept on the benchtop of a fume hood for 10 min, followed by exposure to H_2O (100% humidity in air) in a plastic zippered bag containing an open jar of water for 5 min, followed by removal and placement on the fume hood benchtop for 20 min.

Semiquantitative Detection of NH_3. A sensor tag for 4 ppm NH_3 (**CARD-1B**) was fabricated with $R_s = 19.2 \pm 0.2$ kΩ and a sensor tag for 35 ppm NH_3 (**CARD-1A**) with $R_s = 16.3 \pm 0.5$ kΩ. Before exposure to NH_3 both types of tags were on and readable by the phone (Fig. 3*B* and Fig. S8). Upon exposure to 4 ppm NH_3, **CARD-1B** turned off within 1 min of experiencing a change to its local environment, whereas **CARD-1A** remained on. After 5 min of exposure to 4 ppm NH_3, **CARD-1B** had $R_s = 21.9 \pm 0.4$ kΩ ($\Delta R_s = 2.8 \pm 0.4$ kΩ); **CARD-1A** displayed $R_s = 18.8 \pm 0.3$ kΩ ($\Delta R_s = 2.6 \pm 0.1$ kΩ). The same type of experiment, with a new batch of **CARD-1A** and **CARD-1B**, each fabricated in triplicate, was repeated for 35 ppm NH_3 (Fig. 3*B*). Under these conditions, CARDs turned off ($\Delta R_s = 6.0 \pm 0.5$ kΩ): **CARD-1B** R_s increased to 25.8 ± 0.6 kΩ ($\Delta R_s = 6.3 \pm 0.1$ kΩ), and **CARD-1A** R_s increased to 21.9 ± 0.8 kΩ ($\Delta R_s = 5.4 \pm 0.8$ kΩ), both above the readability threshold.

Determination of Estimated Power Transfer from SGS4 to CARDs. The power transferred from SGS4 to CARD-2 at each stage of fabrication was determined according to a seven-step procedure. (*i*) We collected S_{11} spectra ($n = 5$) (10–20 MHz) of the SGS4-generated signal and averaged them into a single SGS4-signal spectrum. (*ii*) We collected S_{11} spectra ($n = 5$) (10–20 MHz) at each stage of modification of a tag leading to the formation of CARD-2. Additionally we collected S_{11} spectra ($n = 5$) (10–20 MHz) of CARD-2 before and after exposure to saturated cyclohexanone vapor, as described in Fig. 2*A*. (*iii*) We averaged the spectra collected in step *ii* into a single spectrum for each tag modification stage and for the gas exposure scenario. (*iv*) The SGS4-signal spectrum and each spectrum from step *iii* was zeroed according to their response at 20 MHz. (*v*) The zeroed SGS4-signal spectrum from step *iv* was added to each zeroed tag and CARD-2 spectrum from step *iv* to yield SGS4-tag composite spectra (Fig. S6*A*). (*vi*) The power reflected back to the network analyzer, P_{re}, was determined according to Eq. **S1**:

$$S_{11} = 10 \log\left(\frac{P_{re}}{P_{in}}\right), \qquad \textbf{[S1]}$$

where incident power (P_{in}) is 0 dBm (1 μW) (Fig. S6 *B* and *C*). (*vii*) The percent power transferred in each case (P_t) (Fig. 2*B*) was estimated by Eq. **S2** (Fig. S6*C*):

$$P_t(\%) = \left[\frac{\left(\int_{13.53\ MHz}^{13.58\ MHz} P_{re}^{SGS4} df - \int_{13.53\ MHz}^{13.58\ MHz} P_{re}^{x} df\right)}{\int_{13.53\ MHz}^{13.58\ MHz} P_{re}^{SGS4} df}\right] \times 100\%, \qquad \textbf{[S2]}$$

where x corresponds to scenarios 1–6 described in Fig. 2*A* of the main text.

Determination of R_t. The on/off threshold, R_t, was estimated (Table S1) by taking the average of the median R_s values found between the "last" R_s correlated with an unreadable CARD and the "first" R_s correlated with a readable CARD, during recovery from a given exposure to analyte.

1. Mirica KA, Weis JG, Schnorr JM, Esser B, Swager TM (2012) Mechanical drawing of gas sensors on paper. *Angew Chem Int Ed Engl* 51(43):10740–10745.
2. Mirica KA, Azzarelli JM, Weis JG, Schnorr JM, Swager TM (2013) Rapid prototyping of carbon-based chemiresistive gas sensors on paper. *Proc Natl Acad Sci USA* 110(35):E3265–E3270.
3. Michaels RA (1999) Emergency planning and the acute toxic potency of inhaled ammonia. *Environ Health Perspect* 107(8):617–627.
4. Lai H, Leung A, Magee M, Almirall JR (2010) Identification of volatile chemical signatures from plastic explosives by SPME-GC/MS and detection by ion mobility spectrometry. *Anal Bioanal Chem* 396(8):2997–3007.
5. Cox JR, Müller P, Swager TM (2011) Interrupted energy transfer: Highly selective detection of cyclic ketones in the vapor phase. *J Am Chem Soc* 133(33):12910–12913.

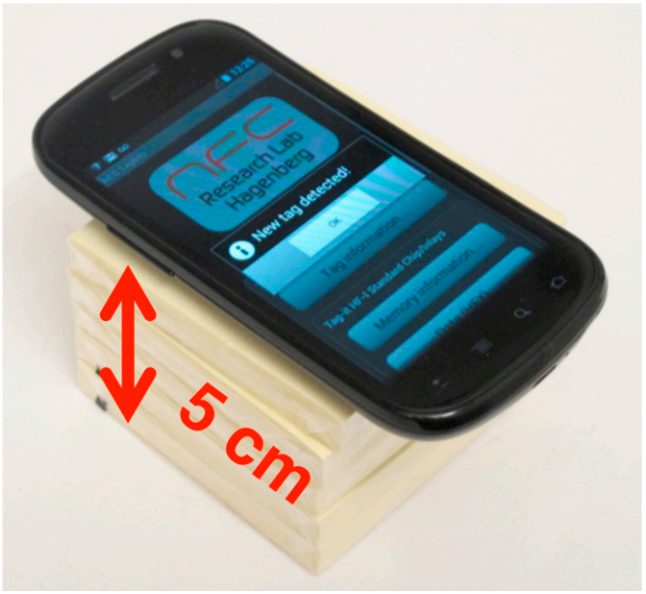

Fig. S1. NFC is a non-line-of sight wireless communication technology. Demonstration of readability of an unmodified tag through sticky notes using Google Nexus S.

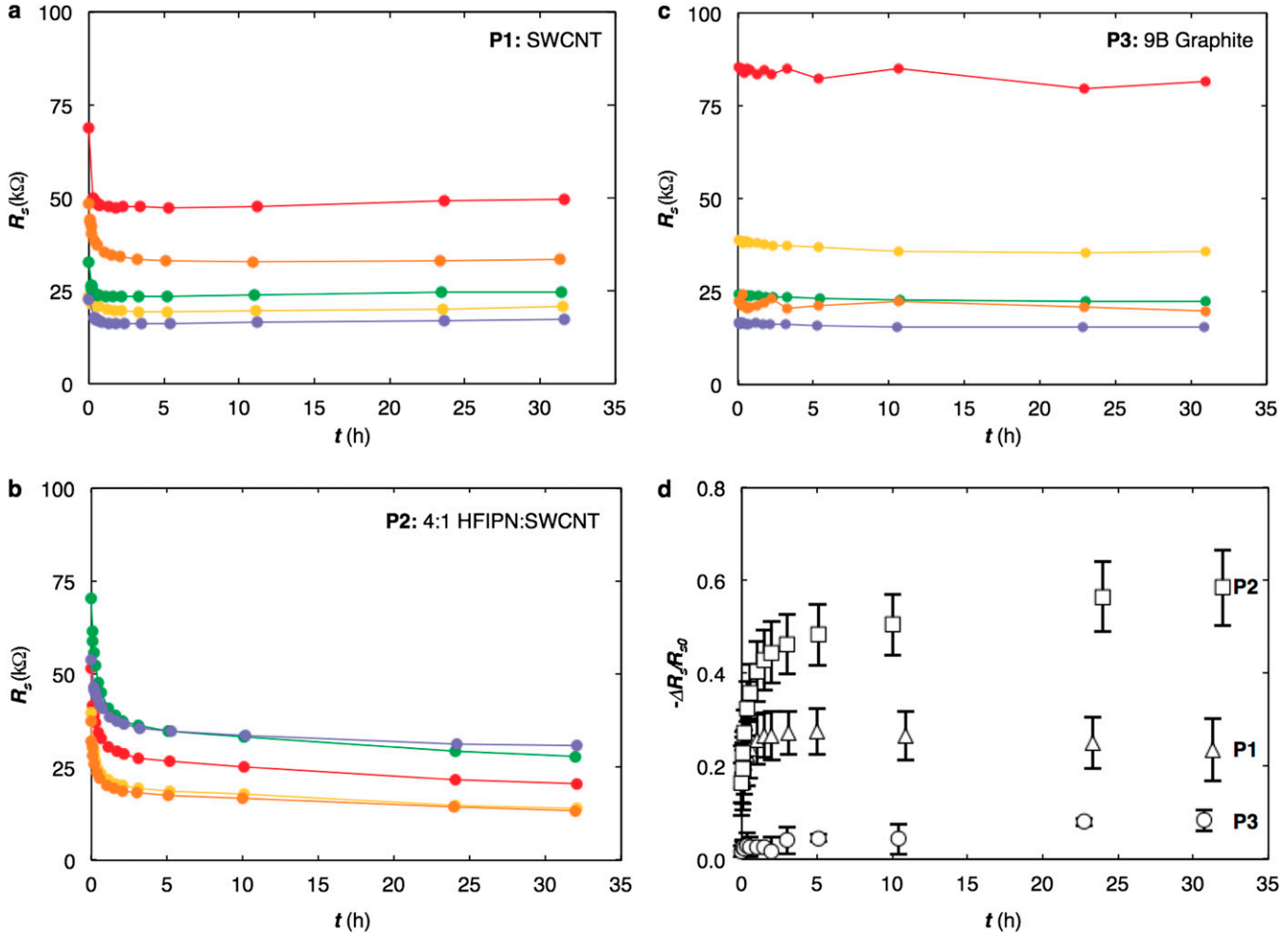

Fig. S2. CARD R_s drifts predictably. CARDs ($n = 5$) made by drawing (*A*) **P1**, (*B*) **P2**, and (*C*) **P3** exhibit predictable drift characteristics across a range of initial R_s values. (*D*) Normalized change in resistance as a function of time for CARDs corresponding to *A* (squares), *B* (triangles), and *C* (circles).

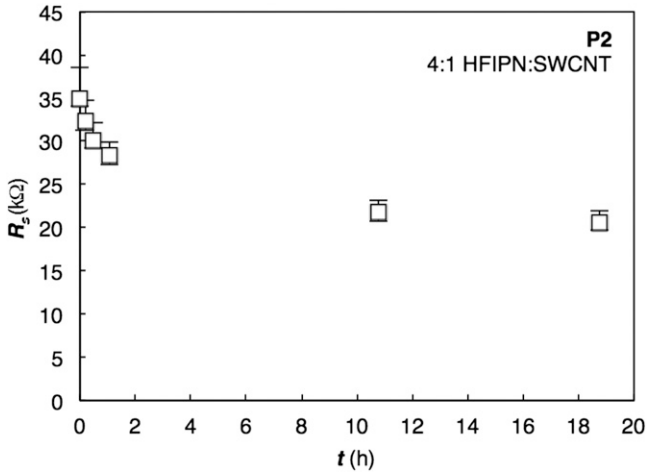

Fig. S3. CARDs can be fabricated to a desired R_s range. R_s drift of **CARD-2** drawn as close to initial $R_s = 35$ kΩ as possible ($n = 9$) with **P2**. Initial average $R_s = 35$ kΩ ± 4 kΩ. Final average $R_s = 21 \pm 1$ kΩ. Error bars represent SD from the average for nine distinct tags.

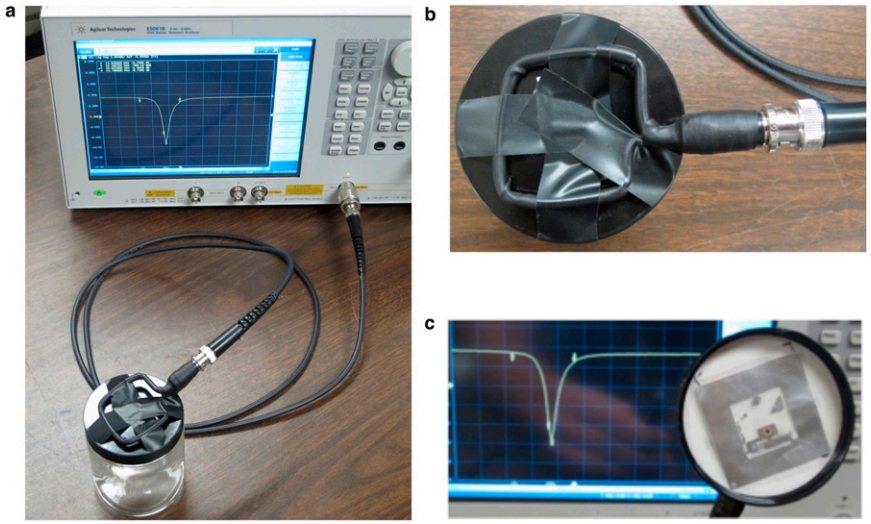

Fig. S4. Radio frequency reflection coefficient (S_{11}) measurements are performed with a loop probe connected to a vector network analyzer. (*A*) Vector network analyzer shown connected to loop probe affixed to a jar cap on an empty jar. (*B*) Image of the custom-made loop probe used in this study, taped to the top of a jar cap with electrical tape. (*C*) Image of a CARD placed on the inside of a jar cap using double-sided tape.

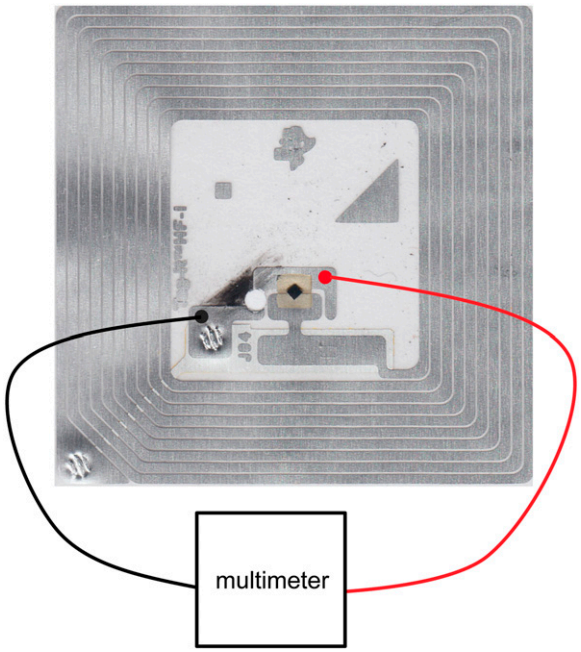

Fig. S5. R_s was measured using a multimeter by contacting the CARD at the locations depicted above.

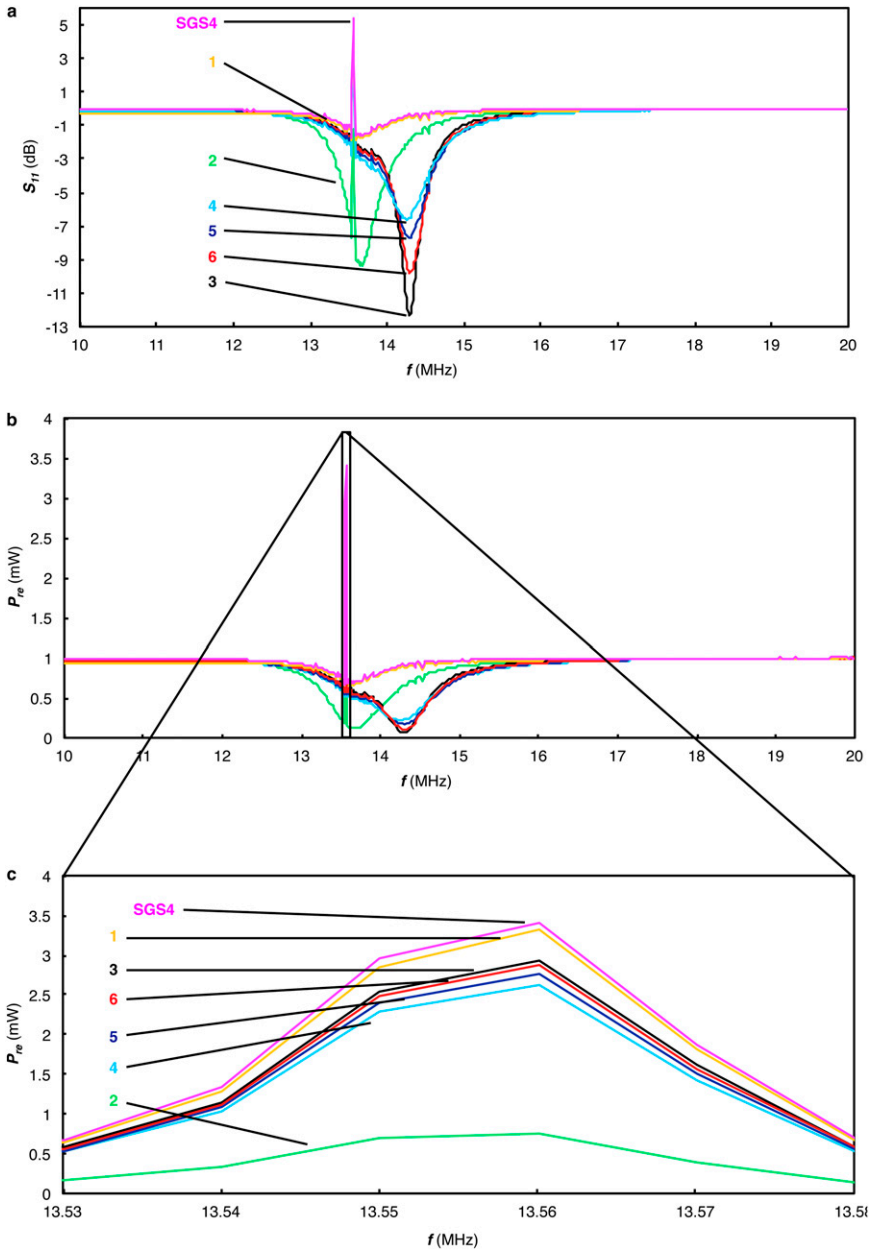

Fig. S6. Procedure for estimating power transfer from SGS4 to an NFC tag or CARD. (*A*) Reflection coefficient (S_{11}) spectrum of SGS4-generated signal (magenta) and spectra of SGS4-generated signal added to spectra of (1) baseline (no tag present), (2) unmodified NFC tag, (3) circuit-disrupted tag, (4) **CARD-2**, and (5) **CARD-2** in the presence of cyclohexanone (equilibrium vapor pressure at ambient temperature and pressure) for 5 s and (6) for 1 min. (*B* and *C*) Original and magnified spectra, respectively, of estimated power received by the network analyzer corresponding to scenarios depicted in *A*.

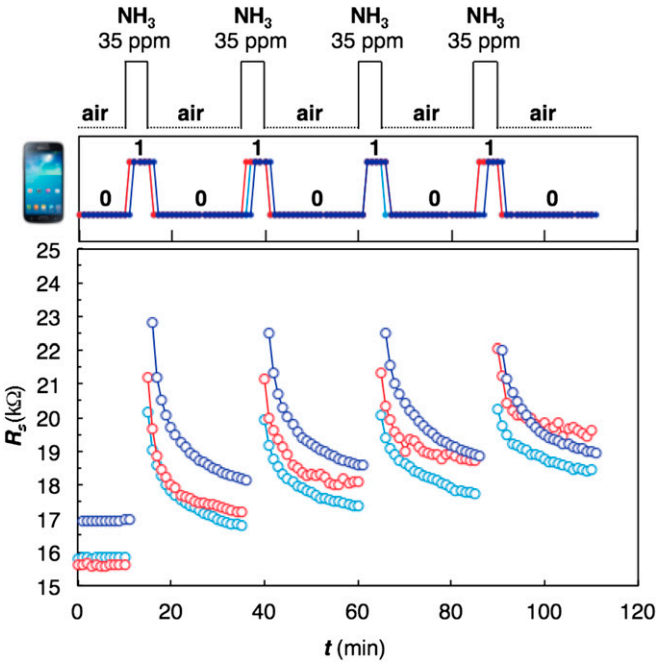

Fig. S7. CARD-1A displays reversible behavior to multiple exposures of NH_3 (35 ppm). Response of CARD-1A ($n = 3$) to four 5-min exposures of NH_3 (35 ppm) at 20-min intervals as monitored with a SGS4 (*Top*, lines) and a multimeter (*Bottom*, open circles).

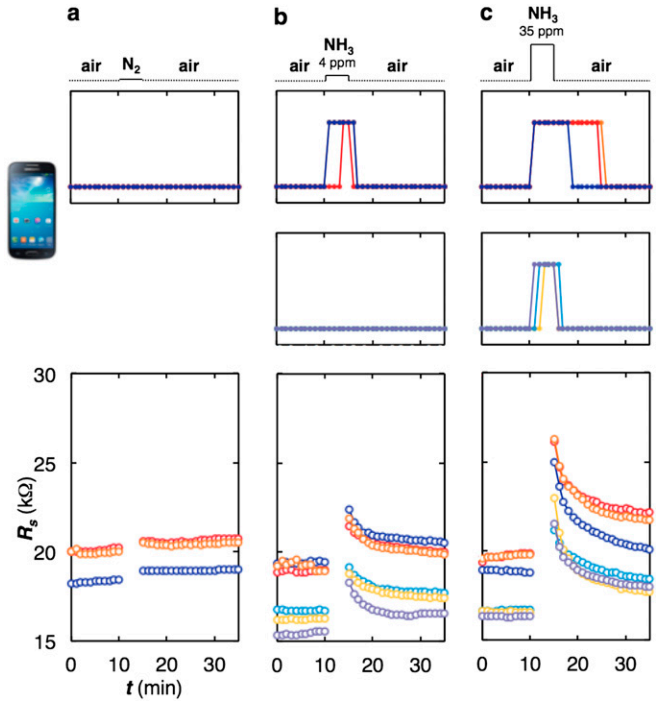

Fig. S8. CARD-1B responds to 4 ppm NH_3 in N_2, but does not respond to pure N_2. (*A*) Response of three distinct **CARD-1B** (dark blue, orange, and red) to a single 5-min exposure of nitrogen as monitored with a SGS4 (*Top*, closed circles) and a multimeter (*Bottom*, open circles). Response of three distinct **CARD-1A** (purple, yellow, and light blue) and **CARD-1B** (dark blue, orange, and red) to a single 5-min exposure of (*B*) 4 ppm NH_3 and (*C*) 35 ppm NH_3 as monitored with a SGS4 (*Top*, closed circles) and a multimeter (*Bottom*, open circles).

Table S1. Estimated R_t of CARDs used in this study

Entry	Fig.	PENCIL	Analyte	*n*	R_t
A	3*A*	**P1**	NH_3	12	20.8 ± 1.0
B	3*B*	**P1**	NH_3	9	21.6 ± 0.7
C	4*A*	**P1**	NH_3	3	20.2 ± 0.5
D	4*B*	**P1**	H_2O_2/H_2O	3	22.4 ± 2.4
E	4*C*	**P2**	$C_6H_{10}O$	3	24.0 ± 1.8

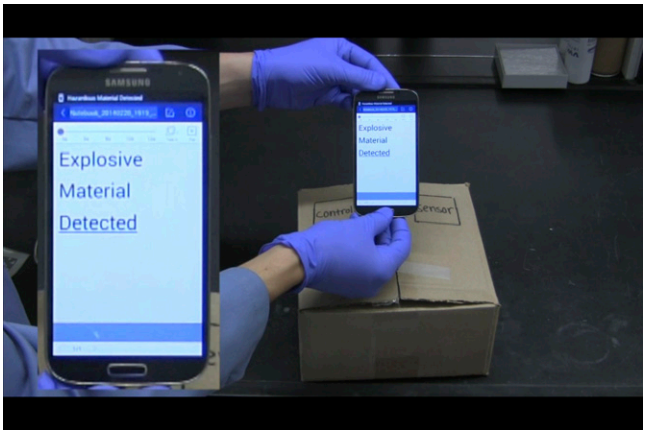

Movie S1. A peroxide-based explosive mimic is detected inside a cardboard box with a GPS-enabled SGS4.

Movie S1